

Supplementary Data:

ANU Argon Facility Technical Report: ANU16-2021

40Ar/39Ar Analysis for National Argon Map

By Marnie Forster and Davood Vasegh

NAM Proposal 17:

Tectonism and Exhumation of the Paterson Orogen and East Pilbara Craton margin

Methods and procedures

Sample selection and mineral separation:

The samples in this study were provided by Geological Survey of Western Australia and the separation procedures were undertaken in rock crushing and mineral separation laboratories at The Australian National University (Table 1). No chemical or leaching treatments were used during separation.

Mineral separation begins by choosing the most pristine sections with no evidence of weathering or staining. For samples with a targeted microstructure, the rock is first sliced into thin slabs using a trim saw, the selected area was then cut from the rock using a band saw. Once the selected area was separated, it was then crushed, milled and de-slimed as many times as was necessary to clean the grains and finally washed in deionised water.

K-feldspar procedure:

For these minerals the grains are sieved into size fractions as mentioned in Table 1 and passed through 0.25A then 1.0A current using a Frantz magnetic separator. K-feldspars are concentrated in the non-magnetic 1A fraction. This grain fraction is then separated under gravity using the Lithium heteropolytungstates (aq) (LST) heavy liquid at 2.58 g/cm³. K-feldspars are concentrated in the lighter than 2.58 g/cm³ size fraction. The separated grains are washed as many times as was necessary to remove any residue LST on the grains with deionised water. Final hand-picking of the best quality grains was done in the Argon Preparation Laboratory.

Muscovite procedure:

For these minerals the grains are sieved into size fractions as mentioned in Table 1. Additional white mica is obtained through 0.25A then 1.0A current using a Frantz magnetic separator. Final hand-picking of the best quality grains was done in the Argon Preparation Laboratory.




Hornblende procedure:

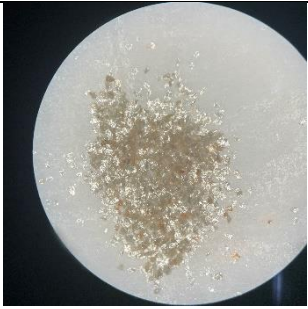
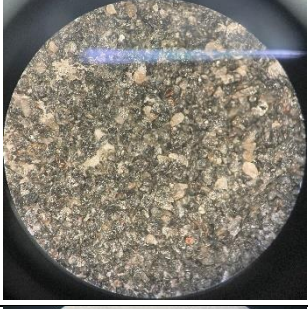

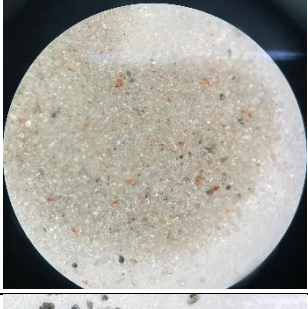
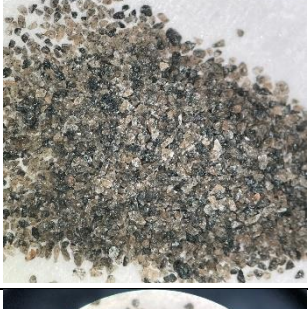
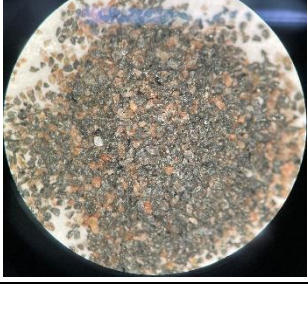
For these minerals the grains are sieved into size fractions as mentioned in Table 1 and passed through 0.25A current using a Frantz magnetic separator. Hornblendes are concentrated in the magnetic 0.25A fraction. If the separates from FRANTZ is not pure (i.e. $\geq 50\%$ hornblende), this grain fraction is then separated under gravity using the Lithium heteropolytungstates (aq) (LST) heavy liquid at 2.9 g/cm³. Hornblendes are concentrated in the heavier than 2.9 g/cm³ size fraction. The separated grains are washed as many times as was necessary to remove any residue LST on the grains with deionized water Final hand-picking of the best quality grains was done in the Argon Preparation Laboratory.


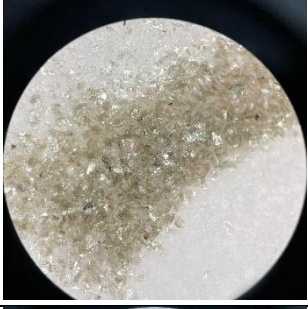
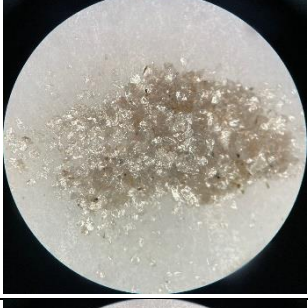
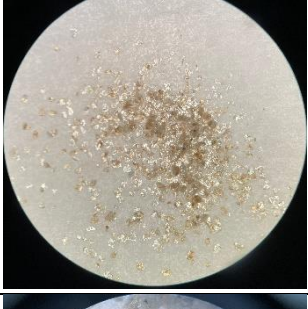
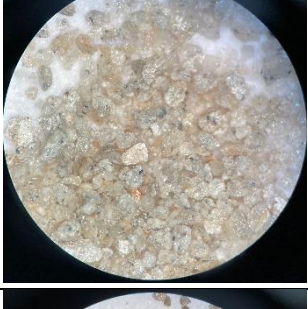
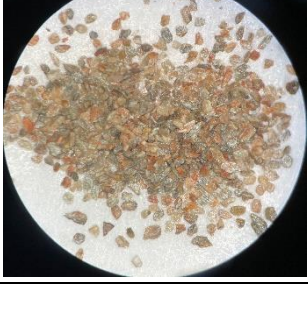
Biotite procedure:

For these minerals the grains are sieved into size fractions as mentioned in Table 1 and paper concentration is performed on the size fraction to obtain the purest mineral separation as possible. Additional biotite is obtained by separating grains through 0.25A current using a Frantz magnetic separator, with biotite concentrated in the magnetic 0.25A fraction. Final hand-picking of the best quality grains was done in the Argon Preparation Laboratory.

Mineral separation details:

Sample ID	Target Mineral	Mass (mg)	Grain Size (μm)	Treatment / Comment	Picture
237172, D01	Biotite	9.3	420-250	Shiny black flaky biotite crystals, pure fraction	
247517, D02	Biotite	9.1	420-250	Shiny black biotite crystals, pure fraction	
237180, D03	Biotite	9.5	420-250	Shiny black flaky biotite crystals, pure fraction	
237196, D04	Biotite	15.7	420-250	Biotite-quartz composite crystals	
237134, D05	Biotite	10.4	420-250	Shiny black biotite crystals, pure fraction	

46920, D06	Muscovite	10.1	420-250	Shiny clean white-mica flakes, pure fraction	
41503, D07	Hornblende	162.6	420-250	Weathered Hbl crystals, clean fraction	
224224, D08	Muscovite	8.9	420-250	White-mica flakes with biotite growths (composites), clean fraction	
114074, D09	Muscovite	8.0	420-250	Clean and thin white-mica flakes in a mixture, clean fraction	
100594, D10	Hornblende	177.5	420-250	Weathered Hbl crystals, clean fraction	
100592, D11	Hornblende	180.4	420-250	Weathered Hbl composite crystals (Hbl-pink qtz)	

247932, D12	Muscovite	7.3	420-250	Clean pristine white-mica grains, pure fraction	
115614, D13	Muscovite	8.7	420-150	Clean pristine white-mica grains, pure fraction	
115629, D14	Muscovite	8.4	420-250	Clean pristine white-mica grains, pure fraction	
115692, D15	Muscovite	9.6	420-250	Clean pristine white-mica grains, pure fraction	
104919, D16	Muscovite	8.7	420-150	white-mica aggregates with minute mafic (Bt/Hbl) inclusions	
109760, D17	Muscovite	8.4	420-250	white-mica aggregates	

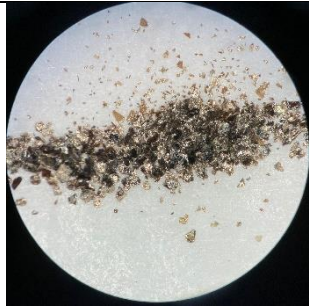
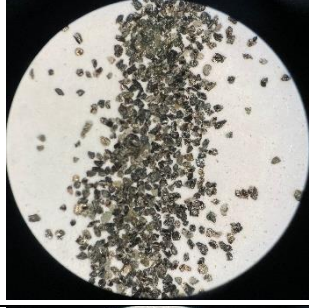
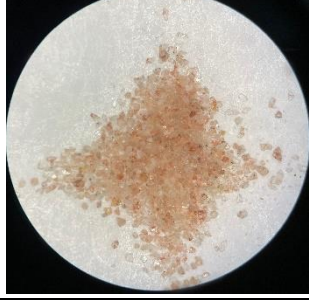
224274, D18	Biotite	9.5	420-250	Shiny black biotite crystals, pure fraction	
224274, D19	Hornblende	173.6	420-250	Clean black hornblende crystals, very rare dirty crystals present, clean fraction	
109759, D20	K-feldspar	10.7	420-250	K-feldspar-Quartz mixture, clean fraction	

Table 1: Mineral separation details

Sample irradiation details:

Irradiation of samples for $^{40}\text{Ar}/^{39}\text{Ar}$ analysis was undertaken at the University of California Davis McClellan Nuclear Research Centre, CA, US in Central Facility position of TRIGA reactor without rotation, with 1.0mm of Cadmium shielding as ANU CAN #38 for 18.0 hours on 23-25 June 2021.

The calculated amounts of grains were weighed and recorded and then wrapped in labelled aluminium packets in preparation for irradiation. The sample filled foils were placed into a quartz irradiation canister together with aliquots of the flux monitor Biotite GA1550. The foil packets of GA1550 standards were dispersed 6-8mm apart throughout the irradiation canister, between the unknown age samples. In addition, packets containing K_2SO_4 and CaF_2 were placed in the middle of the canister to monitor argon isotope production from potassium and other interfering elements.

Irradiated samples were unwrapped upon their return to the Australian National University, and then rewrapped in tin foils in preparation for analysis under vacuum in the furnace. Tin foil is used because the melting temperature of tin is lower than the experiment starting point in the furnace and gasses from tin can be pumped away prior to the sample analysis.

$^{40}\text{Ar}/^{39}\text{Ar}$ procedures and analysis information

Methodology:

Temperature-controlled resistance furnace step-heating experiments is the technique that is used in the ANU Argon laboratory to extract argon isotopes from the samples to ensure 100% release of ^{39}Ar . A sample is dropped into a cleaned furnace and heated to 400°C to melt the tin foil and then left in the furnace at 350°C for 8-12 hours to pump away unwanted gases. This cleaning procedure has proven to significantly improve the quality of the resultant data. The step-heating experiment then

starts at 450°C, and each incremental heating step is heated at a constant temperature for 15 minutes. The heating process involves rapid heating to the setpoint temperature with no overshoot, then temperature is maintained for 15 minutes followed by rapid cooling; this procedure produces a square wave in temperature for each heating step. The heating step schedule for biotite and muscovite rises by 30°C increments (except for the last a few steps), with 30 steps per sample, while K-feldspar is analysed in more than 40 steps, including numerous isothermal steps. Diffusion experiments, as conducted in the ANU Argon laboratory, are designed to retrieve diffusion parameters which can be used in quantitative temperature-time modelling. The heating schedules are recorded in the Excel Tables for each sample.

Cleaning of the furnace between samples is vital in this method. The furnace is degassed four times at 1,450°C for 15 minutes and the gas pumped away prior to the loading of the subsequent sample. Blanks are measured to monitor the cleaning process. The flux monitor crystals are fused using a CO₂ continuous-wave laser. Gas released from either the flux monitors or each step of the sample analyses are exposed to three Zr-Al getters; two AP10 (Cold and hot) and one CP50, each for 10 minutes, to remove active gases. The purified extracted gasses are then isotopically analysed in the Argus VI mass spectrometer. The ⁴⁰Ar/³⁹Ar dating technique is adapted from McDougall and Harrison (1999) and described in Forster and Lister (2009).

Background levels are measured and subtracted from all analyses, from flux monitors and samples. The nuclear interfering values for the correction factors for the isotopes are listed below (Tetley et al 1980). These are measured for the reactions and uncertainties of (³⁶Ar/³⁷Ar)_{Ca}, (³⁹Ar/³⁷Ar)_{Ca}, (⁴⁰Ar/³⁹Ar)_K, (³⁸Ar/³⁹Ar)_K and (³⁸Ar)_{Cl}/^{(39)Ar_K, and were calculated prior to sample analyses.}

Mass spectrometer setup and procedures

Samples and standards were analysed in the Argon Laboratory at the Research School of Earth Science, The Australian National University, Canberra, Australia using a *Thermo Fisher ARGUS-VI* multi-collector mass spectrometer (Table 2).

Mass Spectrometer:	Thermo Fisher Argus VI
Detector Type:	Faraday Cups only x5
Calibrations:	3 levels (Zero Offset, Gain and Cross Calibration)
Peak Centring:	Once for every measurement @H2 (⁴⁰ Ar)
Measurement Cycles:	51 cycles on all detectors
Extrapolation Method:	Exponential extrapolation and uncertainty

Name	UFC Offset [fA]	Gain	Cross Calibration Factor
H2	-4.9761469	0.9871203	1
H1	-2.2071069	0.9671459	1.007184188
AX	-7.6814703	0.9769602	1.017518151
L1	-2.3979322	0.9706487	1.030604297
L2	-3.1329948	0.9676338	1.047244337

Table 2: Detector Calibration Values

The calculation parameters:

Lambda ⁴⁰ K (Renne et al 2011)	5.5305E-10
Lambda ³⁷ Ar (Kondev et al 2017)	1.9798E-02
Lambda ³⁹ Ar (Kondev et al 2017)	7.0548E-06
Lambda ³⁶ Cl (Kondev et al 2017)	6.2985E-09
Flux Monitor	GA1550 @ 99.18 ± 0.14 Ma

Total irradiation power 18.00 MW
 Irradiation Date 23-25 Jun, 2021
 Irradiation shielding Cadmium 1.0mm

Interfering isotope production ratios:

$(^{36}\text{Ar}/^{37}\text{Ar})_{\text{Ca}}$ correction factor 1.96095E-04
 $(^{39}\text{Ar}/^{37}\text{Ar})_{\text{Ca}}$ correction factor 8.53577E-04
 $(^{40}\text{Ar}/^{39}\text{Ar})_{\text{K}}$ correction factor 2.68686E-01
 $(^{38}\text{Ar}/^{39}\text{Ar})_{\text{K}}$ correction factor 1.15556E-02
 $(^{38}\text{Ar})_{\text{Cl}}/(^{39}\text{Ar})_{\text{K}}$ correction factor 8.04746E-02
 Ca/K conversion factor 1.90

Atmospheric Argon correction ratio:

$^{40}\text{Ar}/^{36}\text{Ar}$ (Lee et al 2006) 298.57
 $^{40}\text{Ar}/^{38}\text{Ar}$ (Lee et al 2006) 1,583.52

Representative air shot and blanks measurements:

The discrimination factor was calculated by analysing five air shots analysis on either side of sample analysis and the calculation of the 1amu was used for the discrimination factor. Table 3 shows an example of the analysed air shots.

Date	$^{40}\text{Ar} \pm \%err$		$^{38}\text{Ar} \pm \%err$		$^{36}\text{Ar} \pm \%err$		1amu $\pm \%err$		Reported Value
03-Sep-2021	1,974.486	0.015	1.252	1.593	6.633	0.275	1.00076	0.147	1.0006465 \pm 0.107%
03-Sep-2021	1,972.593	0.015	1.256	1.582	6.644	0.337	1.00140	0.177	
03-Sep-2021	1,971.383	0.013	1.237	1.527	6.615	0.307	1.00048	0.162	
03-Sep-2021	1,968.652	0.013	1.240	1.476	6.610	0.292	1.00063	0.155	
03-Sep-2021	1,968.284	0.013	1.242	1.487	6.591	0.296	0.99996	0.157	

Table 3: Air Shots and Mass Discrimination Factor

The blank measurements are undertaken with different temperatures schedule between 300°C and 1450°C, depending on the degassing behaviour and previous blank measurement results. The degassing and blank measurement procedure continues until the ratios of ^{40}Ar , ^{38}Ar and ^{36}Ar drop to atmospheric ratios, and ^{39}Ar and ^{37}Ar drop below detectable levels. The entire procedure of degassing and blank measurements is repeated at the end of a set of samples. Blanks will be done in-between samples that belong to a set, with reduced steps at 300°C, 1300°C and 1450°C to check isotope levels. In addition, the mass of each sample is calculated so that the volume of gas released from each step overwhelms the volume of gas that may occur in the blank. The table 4 is a representative sequence of measured blank values recorded during a monitoring process.

Temperature	^{40}Ar	^{39}Ar	^{38}Ar	^{37}Ar	^{36}Ar	$^{40}\text{Ar}/^{36}\text{Ar}$
300	1817.738	0.708661	1.209615	ND*	6.113996	297.3077
500	1879.391	0.741332	1.266375	ND	6.364901	295.2743
700	1911.306	0.759696	1.282523	0.095807	6.417252	297.8386
900	2053.27	0.775687	1.358664	ND	6.94095	295.8198
1100	2731.788	0.812587	1.788944	0.10454	9.192207	297.1852
1300	7305.089	1.038774	4.728446	0.139915	24.59727	296.9878
1450	36811.09	2.436249	23.78145	0.23653	124.4077	295.8909
300	748.5261	0.344558	0.467985	0.019884	2.5069	298.5864
1300	1126.281	0.438838	0.704102	0.0207706	3.744338	300.7958
1450	2181.428	1.00614	1.377076	0.1028531	7.299197	298.8587

Table 4: Example of the blanks measurements during a sequence of blanks where isotopes were being monitored prior to sample analysis (* => Not Detectable). Temperature is °C.

Data reduction software:

The calculations were done with an adapted version of *Noble* Software (2022, developed and adapted by the Australian National University Argon Laboratory) and all interpretation have been undertaken with *eArgon* (developed and adapted for ANU Argon Laboratory by G.S. Lister).

Reported Data:

The reported data have been corrected for system backgrounds, mass discrimination, fluence gradients and atmospheric contamination. GA1550 standards were analysed, and an exponential best fit was then used for the calculation of the J-factor and J-factor uncertainty (Table 5).

Samples J-Factor, Mass Discrimination, and uncertainties:

Sample Name	J-Factor \pm %uncertainty		Mass Discrimination Factor \pm %uncertainty		Measurement Date
237172, D01	3.29177E-03	0.1851	1.00133	0.094	20-Aug-2021
247517, D02	3.29145E-03	0.1851	1.00180	0.087	23-Aug-2021
237180, D03	3.29113E-03	0.1851	1.00180	0.087	26-Aug-2021
237196, D04	3.29081E-03	0.1851	1.00180	0.087	28-Aug-2021
237134, D05	3.29049E-03	0.1851	1.00180	0.087	29-Aug-2021
46920, D06	3.29004E-03	0.1851	1.00180	0.087	30-Aug-2021
41503, D07	3.28992E-03	0.1851	1.00201	0.113	01-Sep-2021
224224, D08	3.28979E-03	0.1851	1.00065	0.107	03-Sep-2021
114074, D09	3.28966E-03	0.1851	1.00065	0.107	05-Sep-2021
100594, D10	3.28921E-03	0.1851	1.00189	0.109	06-Sep-2021
100592, D11	3.28890E-03	0.1851	1.00115	0.102	18-Oct-2021
247932, D12	3.28858E-03	0.1851	1.00115	0.102	21-Oct-2021
115614, D13	3.28842E-03	0.1851	1.00115	0.102	23-Oct-2021
115629, D14	3.28826E-03	0.1851	1.00115	0.102	25-Oct-2021
115692, D15	3.28810E-03	0.1851	1.00115	0.102	27-Oct-2021
104919, D16	3.28784E-03	0.1851	1.00171	0.084	08-Nov-2021
109760, D17	3.28778E-03	0.1851	1.00187	0.114	06-Nov-2021
224274, D18	3.28768E-03	0.1851	1.00187	0.114	04-Nov-2021
224274, D19	3.28762E-03	0.1851	1.00101	0.071	01-Nov-2021
109759, D20	3.28746E-03	0.1851	1.00101	0.071	29-Oct-2021

Table 5: Sample analysis and calculation details

$^{40}\text{Ar}/^{39}\text{Ar}$ isotopic data of the samples are supplied in the Excel Data Tables, which include details on the heating schedule, Argon isotopes abundances and their uncertainty levels, %Ar*, $^{40}\text{Ar}^*/^{39}\text{Ar}(\text{K})$, Cumulative $^{39}\text{Ar}\%$, calculated age and its uncertainty, Ca/K, Cl/K, J-Factor and its uncertainty. Noting that all the reported uncertainties are at one sigma level and the fractional uncertainties are shown as % in the headings of the appropriate columns of data tables. The components involved in the calculation of the uncertainties have listed in Table 6.

Uncertainty of:	Components involved in the calculation
Isotope Abundances	Uncertainty of isotope measurement Uncertainty of Mass Discrimination Factor (except for ^{39}Ar)
J-Factor	Uncertainty of ^{40}K Decay Constant Uncertainty of Age of the Flux monitor Uncertainty of Flux monitor isotopes abundances
Calculated Age	Uncertainty of Isotopes Abundances J-Factor value and uncertainty of J-Factor ^{40}K Decay Constant value and uncertainty of ^{40}K Decay Constant

Table 6: Components involved in the calculation of each uncertainty

References:

Forster, M.A. and Lister, G.S. 2004. The interpretation of $^{40}\text{Ar}/^{39}\text{Ar}$ apparent age spectra produced by mixing: application of the method of asymptotes and limits. *Journal of Structural Geology* 26, 287–305

Forster, M.A. and Lister, G.S. 2009. Core-complex-related extension of the Aegean lithosphere initiated at the Eocene-Oligocene transition. *Journal Geophysical Research*, 114, B02401.

Kondev, F.G. and Naimi, S. 2017. The NUBASE2016 evaluation of nuclear properties. *Chinese physics C*, 41(3), p.030001.

Lee, J.Y., Marti, K., Severinghaus, J.P., Kawamura, K., Yoo, H.S., Lee, J.B. and Kim, J.S. 2006. A redetermination of the isotopic abundances of atmospheric Ar. *Geochimica et Cosmochimica Acta*, 70(17), 4507-4512.

McDougall, I. and Harrison, T.M. (Eds.). 1999. *Geochronology and Thermochronology by the $^{40}\text{Ar}/^{39}\text{Ar}$ Method*, 2nd ed., 269 pp. Oxford Univ. Press, New York.

Renne, P.R., Balco, G., Ludwig, K.R., Mundil, R. and Min, K., 2011. Response to the comment by WH Schwarz et al. on “Joint determination of ^{40}K decay constants and $^{40}\text{Ar}^*/^{40}\text{K}$ for the Fish Canyon sanidine standard, and improved accuracy for $^{40}\text{Ar}/^{39}\text{Ar}$ geochronology” by PR Renne et al.(2010). *Geochimica et Cosmochimica Acta*, 75(17), pp.5097-5100.

Spell, T. L. and I. McDougall. 2003. Characterization and calibration of $^{40}\text{Ar}/^{39}\text{Ar}$ dating standards. *Chemical Geology*, 198, 189–211.

Tetley, N., McDougall, I. & Heydegger, H.R. 1980. Thermal neutron interferences in the $^{40}\text{Ar}/^{39}\text{Ar}$ dating technique. *Journal Geophysical Research*, 85, 7201–7205.